Frontiers in Bioscience Landmark

Front. Biosci. (Landmark Ed) **2026**; 31(5): 48867
https://doi.org/10.31083/FBL48867

Short Communication

Immunomodulatory Effect of Aza-Spirocyclic Frameworks

Anjali Prajapati[1,2], Rajitha Rajeshwar Tatikonda[1,2], Raji Reddy Chada[2,3,*], Srinivasa Reddy Bonam[1,2,*]

[1]Vaccine Immunology Laboratory, Department of Applied Biology, CSIR-Indian Institute of Chemical Technology, 500007 Hyderabad, Telangana, India
[2]Academy of Scientific and Innovative Research (AcSIR), 201002 Ghaziabad, India
[3]Department of Organic Synthesis & Process Chemistry, CSIR-Indian Institute of Chemical Technology, 500007 Hyderabad, Telangana, India
*Correspondence: rajireddy@iict.res.in (Raji Reddy Chada); bonamsr.iict@csir.res.in; bsrpharmacy90@gmail.com (Srinivasa Reddy Bonam)
Academic Editor: Changqing Su
Submitted: 6 December 2025 Revised: 2 April 2026 Accepted: 14 April 2026 Published: 18 May 2026

Abstract

Background: Immunomodulators play a central role in the treatment of cancer and immune-mediated disorders. Small-molecule immunomodulators are particularly attractive due to their structural diversity, pharmacological versatility, and potential for oral administration. This study aimed to investigate the immunomodulatory potential of newly synthesized aza-spirocyclic derivatives. **Methods**: A series of novel aza-spirocyclic compounds was evaluated for cytotoxicity in RAW264.7 murine macrophages. Immunomodulatory activity was assessed by quantifying nitric oxide (NO) production and profiling pro- and anti-inflammatory cytokines in macrophages and murine splenocytes. *In vitro* anti-inflammatory effects were further examined using a lipopolysaccharide (LPS)-induced inflammation model. Mechanistic insights were explored using molecular docking and immuno-informatics analyses. **Results**: All compounds were non-toxic at the tested concentrations. Most derivatives failed to induce NO production, indicating an absence of danger-associated molecular pattern (DAMP)-like activity. Several compounds significantly reduced the pro-inflammatory cytokine interleukin-6 (IL-6) while increasing the anti-inflammatory cytokine IL-10 *in vitro*. In the LPS-induced inflammation model, four compounds notably suppressed IL-6 and enhanced IL-10 expression. The binding affinities obtained from docking, along with *in vitro* validation of these compounds on Janus kinases (JAKs) signaling, suggested that compounds **AS8** and **AS10** modulated inflammatory signaling pathways. **Conclusion**: The synthesized aza-spirocyclic derivatives exhibit promising anti-inflammatory profiles, characterized by IL-6 suppression and IL-10 enhancement. These findings position aza-spirocyclic scaffolds as candidates for the development of next-generation small-molecule immunomodulators.

Keywords: aza compounds; immunologic; anti-inflammatory agents; cytokines; janus kinase inhibitors

1. Introduction

Immunomodulators are prophylactic or therapeutic agents, derived from natural or synthetic, that regulate immune system activity either by enhancing immune responses (immunostimulation) or suppressing them (immunosuppression). The development of novel small-molecule immunomodulators holds considerable promise for the treatment of autoimmune disorders, chronic inflammatory diseases, and cancer, as well as for use as vaccine adjuvants. Among the chemical scaffolds explored, derivatives of aza-spirocycles have drawn ample interest because of their broad spectrum of biological activity and physical properties [1]. Moreover, spirocyclic frameworks have emerged as a valuable design strategy in bioactive small molecules, enabling enhanced molecular complexity, improved physicochemical properties, and refined modulation of biological activity. Aza-spirocycles represent an important class of heterocyclic frameworks, widely recognized for their presence in numerous pharmacologically active compounds [2]. The immunomodulatory potential of aza-spirocyclic compounds can be attributed to their capacity to interact with key molecular targets involved in immune regulation, such as cytokine signaling pathways, transcription factors (e.g., NF-κB, STATs, and others), and pattern recognition receptors [e.g., Toll-like receptors (TLRs), NOD-like receptors (NLRs)]. Structural modifications at the spiro junction and benzimidazole core allow fine-tuning of lipophilicity, steric configuration, and hydrogen-bonding potential, which can significantly influence target binding and pharmacokinetic behavior [3]. Such a structure-activity-driven approach provides a rational basis for discovering new immunotherapeutic molecules. In this study, we evaluated two distinct classes of aza-spirocyclic molecules synthesized by our group for their immunomodulatory activity, with the aim of identifying promising candidates for development as small-molecule immunotherapeutics and/or vaccine adjuvants.

2. Materials and Methods

2.1 Aza-Spirocyclic Compounds Synthesis

The aza-spirocyclic compounds were synthesized using the recently developed *ipso*-annulation reactions [4, 5]. In the first case, radical-promoted *ipso*-annulation using aryl sulfonates or AgSCN or $AgSCF_3$ in the pres-

ence of ceric ammonium nitrate (CAN) as an oxidant, provided thio-functionalized (SO_2Ar or SCN or SCF_3) spirocycles in good yields [4]. Next, selenylated azaspirocycles were prepared *via* electrophilic *ipso*-annulation using diphenyl diselenide/$FeCl_3$ reaction conditions. Accordingly, spirocycles **AS1** to **AS6** were obtained from the reaction of *N*-benzylacrylamides induced by *S*-centered radicals (SCN/SCF_3/SO_2Ar) in the presence of CAN as an oxidant. Next, the chalcogenated (SCN/SCF_3/SePh) benzimidazo-fused azaspiro[5,5]undecatri-enones **AS7** to **AS12** were synthesized by the reaction of *N*-propiolyl-2-arylbenzimidazoles involving both the radical-based and electrophilic reactions. All the general synthetic strategies (Scheme S1 & S2) are provided in the **Supplementary Information** along with the analytical data (^{1}H NMR, ^{13}C NMR & mass) along with the HPLC data for the representative compounds.

2.2 Cytotoxicity Assay

The cell line was obtained from the National Centre for Cell Science (NCCS, Pune, India). All cell lines supplied by NCCS were authenticated using Short Tandem Repeat (STR) profiling and tested for mycoplasma contamination [6]. RAW264.7 cells were maintained in Dulbecco's Modified Eagle Medium (DMEM) (AT241-1L, Grand Island, NY, USA) medium supplemented with 10% fetal bovine serum (FBS) (Gibco-16170078) and 1% Penicillin-Streptomycin (Pen-Strep) (Gibco-15140-122, Thermo Fisher Scientific, Grand Island, NY, USA) solution under standard conditions of 37 °C and 5% CO_2 for 24 hours. Cells were cultured in T75 flasks containing 10 mL of media. Then, cells were counted using a haematocytometer. Ten thousand cells per well were cultured in 96-well plates for 24 hours under optimum conditions. Also, compounds were serially diluted in culture media starting with 100 µM up to 0.8 µM concentration. Then, cells were treated with decreasing concentrations of the compounds and incubated for 24 hours at 37 °C and 5% CO_2. Control wells contained only untreated cells. Following 24 hours of incubation, 50 µL of 3-(4,5-dimethylthiazol-2-yl)-2,5-diphenyltetrazolium bromide (MTT) (Sigma, M5655, Milwaukee, WI, USA) solution (5 mg/mL concentration in PBS) was added into each well and incubated for 4 hours at 37 °C and 5% CO_2 for 24 hours. Later, ~100 µL of media was aspirated and discarded, and formazan crystals were dissolved in 50 µL of dimethyl sulfoxide (DMSO) and incubated for 15 minutes. Absorbance (O.D.) was then measured at 570 nm using a microplate reader (MEGALLAN, Tecan Life Sciences, Männedorf, Switzerland). Percentage cell viability was then calculated based on the compound treatment's absorbance relative to the cell control's absorbance [7].

2.3 Nitric Oxide Assay

RAW264.7 cells were maintained as mentioned in the above section. Cells were counted using a haematocytometer, approximately 0.5×10^6 cells per well were seeded in 1 mL in 24-well plates for 24 hours under optimum conditions. After incubation, 100 µM, 10 µM, and 1 µM of each compound and 100 ng/mL of Lipopolysaccharide (LPS) were added to the cells and incubated for 24 hours at 37 °C with 5% CO_2. Supernatant from the cultures was collected and estimated for NO production. The standard was prepared by serial dilution of $NaNO_2$ starting from 100 µM up to 8 times in autoclaved water. 100 µL Griess reagent (Sigma, G4410-10G) was then added to a 96-well plate and incubated for 30 minutes, then absorbance (O.D.) was measured at 545 nm using a microplate reader (MEGALLAN, Tecan Life Sciences). NO production was then calculated based on the compounds' treatment absorbance relative to the standard's absorbance *via* the linear curve method [8].

2.4 Mouse Splenocytes Stimulation

Animal experiments were approved by the Institutional Animal Ethics Committee (IEAC) of the Council of Scientific & Industrial Research, Indian Institute of Chemical Technology (CSIR-IICT). Three C57BL/6 mice were acquired from the internal animal house facility (CSIR-IICT, Hyderabad) and used for isolating spleens for immunological study (IAEC approval number: IICT-IAEC-069-2025). Mice (6–8 weeks old, female) were sacrificed with cervical dislocation, and the spleen was dissected carefully. Splenocytes were isolated by using Ammonium-Chloride-Potassium (ACK) lysis buffer [prepared in the lab]. Later, cells were counted, and approximately 1×10^6 cells per well were seeded in 1 mL in 24-well plates and treated with 100 µM and 10 µM compound, and incubated at 37 °C with 5% CO_2 for 24 hours under optimum conditions. Cell supernatant was then collected for cytokine estimation [9].

2.5 Cytokine Estimation

Secreted cytokines were measured by sandwich enzyme-linked immunosorbent assay (ELISA). For this, RAW264.7 cells and Splenocytes (0.5×10^6 and 1×10^6 cells, respectively) were cultured in a 24-well tissue culture plate in a complete medium (as mentioned earlier) and incubated for 24 hours under standard conditions. Cells were then treated with immunomodulatory compounds at the desired concentration and incubated at 37 °C with 5% CO_2 for 24 hours. In some experiments, cells were pretreated with LPS (100 ng/mL) for 2 hours to induce an inflammatory condition prior to compound treatment. Culture supernatants were then collected and centrifuged at 1500 rpm for 5 minutes to remove any cell debris. IL-6 [BD OPt ELISA, Cat No.- 555240, San Diego, CA, USA], IL-10 [Invitrogen, 88-7105-88, Grand Island, NY, USA], and TNF-α [BD OPt ELISA, Cat No.- 555268, San Diego, CA, USA] in super-

natants were then measured using the ELISA kits following the manufacturer's protocol [10].

2.6 Molecular Docking and Identifying Key Interactions

Molecular docking was performed using AutoDock Vina (Center for Computational Structural Biology, Scripps Research, La Jolla, CA, USA; https://vina.scripps.edu/) [11,12], which employs a scoring function that combines empirical and knowledge-based terms to estimate the binding affinity between ligands and the protein. It utilizes a gradient-based optimization algorithm to efficiently explore the ligand's binding conformations. The 2D structures of the **12** compounds were obtained using ChemDraw (Revvity Signals Software, Inc., Waltham, MA, USA), and their 3D structures were generated with OpenBabel (http://openbabel.org). The experimental crystal structures of JAK1 kinase (PDB: 6N7A) [13], an isoquinoline derivative inhibitor with JAK2 kinase (PDB: 2B7A) [14], and JAK3 (PDB: 5LWM) [15] in complex with a pyrazolopyridine inhibitor and TYK2 (PDB: 6AAM) in complex with peficitinib were considered as starting structures for docking. The protein structures were processed by modeling missing residues, removing all heteroatoms and co-crystal ligands, and converting them to the required PDBQT format using Mgltools. All compounds were also converted to PDBQT format. The binding site was defined by obtaining the center of mass of the respective co-crystal ligand for each JAK isoform. The exhaustiveness parameter was set to the default value of 8. The docking results were visualized with UCSF Chimera, and interaction analysis was performed using BIOVIA Discovery Studio (2024, Dassault Systèmes BIOVIA, San Diego, CA, USA).

2.7 Western Blotting

The mouse macrophages (RAW264.7) cells were seeded in a 12-well plate at a density of 1×10^6 cell/well. After overnight incubation, cells were treated with 100 µM potential JAK inhibitors (**AS1**, **AS2**, **AS8**, and **AS10**), LPS (100 ng/mL), Filgotinib (100 µM), and Momelotinib (50 µM), either with or without LPS stimulation for 2 hours. After 24 hours, cells were lysed using 1× RIPA buffer containing protease and phosphatase inhibitors to extract the protein. The protein concentration was estimated using a BCA kit, and an equal amount (30 µg) of protein was loaded and resolved in 10% SDS-PAGE. The separated proteins were transferred to the nitrocellulose membrane and blocked with 5% BSA for 1 hour. Following blocking, the membrane was incubated with appropriate primary antibodies overnight at 4 °C. After washing three times with 1× TBST, an HRP-conjugated secondary antibody was added and incubated for 2 hours. The signals were developed using an ECL solution, and the bands were visualized and quantified using the ChemiDoc imaging system.

2.8 Statistical Analysis

Data were analysed using GraphPad Prism 8 (GraphPad Software, LLC, San Diego, CA, USA). Comparison of two groups was performed by Student's *t*-test, an unpaired, non-parametric test, and the Mann-Whitney test.

3. Result

3.1 Compounds Characterization

The azaspirocyclic framework is a structural motif found in various natural and synthetic molecules known for their significant pharmacological activities [16]. In addition, thio- and seleno-functionalized molecules are valuable in medicinal chemistry because sulfur and selenium introduce distinctive electronic and redox properties that considerably modify the pharmaceutical properties. These groups can improve lipophilicity, metabolic stability, and target interactions, while offering useful bioisosteric options for tuning potency and selectivity [17]. In light of the favorable properties associated with this class of molecules, we have developed an efficient protocol to access a series of thio-functionalized azaspiro[4,5]decatrienones *via* the dearomative *ipso*-annulation of unactivated N-benzyl acrylamides, induced by S-centered radicals ($SCN/SCF_3/SO_2Ar$) in the presence of CAN as an oxidant [4]. Later, we reported an *ipso*-carbocyclization of N-propiolyl-2-arylbenzimidazoles leading to chalcogenated (SCN/SCF_3/SePh) benzimidazo-fused azaspiro[5,5]undecatrienones in good yields, involving both radical-based and electrophilic pathways [4, 5]. Having developed these two *ipso*-annulation strategies to synthesize both the azaspiro[4,5]decatrienone and azaspiro[5,5]undecatrienone frameworks bearing chalcogenated (S/Se) functionalities, we became interested in investigating their immunomodulatory effects. In particular, the benzimidazole-fused azaspiro[5,5]undecatrienones incorporate two high-value pharmacophoric motifs within a single molecular framework. These motifs are widely represented in bioactive small molecules allied with diverse pharmacological activities, thereby underscoring the potential relevance of these hybrid structures. In addition, the chalcogen-functionalized azaspirocycles obtained through our synthetic strategy provide promising structural templates for medicinal chemistry optimization. Their unique combination of rigidity, three-dimensionality, and heteroatom incorporation positions them as attractive candidates for future drug-discovery and lead-generation efforts (**Supplementary Table 1)**.

3.2 Cytotoxicity of Spirocyclic Compounds to Murine Macrophages

The cytotoxic potential of the spirocyclic compounds (**Supplementary Table 1**) was evaluated in murine macrophages using a colorimetric assay based on the reduction of 3-[4,5-dimethylthiazol-2-yl]-2,5-diphenyltetrazolium bromide (MTT) by mitochondrial dehydrogenases, leading to the formation of blue formazan crys-

tals. All tested compounds preserved cell viability above 90% across concentrations up to 100 µM. None of the compounds exhibited measurable cytotoxicity within this range, and the half-maximal inhibitory concentration (IC_{50}) values were estimated to be greater than 1000 µM (**Supplementary Table 2**), indicating a favorable safety profile for *in vitro* studies.

3.3 Effect of Spirocyclic Compounds on Nitric Oxide and Cytokine Production in Murine Macrophages

The impact of spirocyclic compounds on reactive nitrogen species (RNS) production was assessed using a nitric oxide (NO) assay in RAW264.7 macrophages. None of the tested compounds induced NO production, however, a few of the compounds showed slightly higher NO, although it was not significant. These findings indicate that the spirocyclic compounds do not function as danger-associated molecular pattern (DAMP) or pathogen-associated molecular pattern (PAMP) inducers (Fig. 1A). To further investigate their immunomodulatory potential, culture supernatants from treated macrophages were analyzed for inflammatory cytokine secretion, specifically interleukin-6 (IL-6) and interleukin-10 (IL-10) (Fig. 1B,C), using a sandwich ELISA. IL-6 production remained largely unchanged across treatments, with the exception of compound 1, which elicited a modest increase compared to the cell control. In contrast, IL-10 secretion was significantly elevated in a dose-dependent manner following treatment with the spirocyclic compounds (**AS1**, **AS2**, **AS3**, **AS4**, **AS5**, **AS6**, **AS8**, **AS9**, and **AS10**), suggesting an anti-inflammatory skewing of the compound on macrophage response. Also, LPS induced the significant IL-10 secretion, which may be due to a response of anti-inflammatory macrophages that usually appear at the late stage of LPS stimulation (after 24 hours) [18].

3.4 Aza-Spirocyclic Compounds Elicit Anti-Inflammatory Response in Murine Splenocytes and Murine Macrophages

The impact of spirocyclic compounds on cytokine secretion by murine splenocytes was assessed by quantifying IL-6 and tumor necrosis factor-alpha (TNF-α) levels following treatment. Overall, compound exposure did not enhance pro-inflammatory cytokine production; instead, both IL-6 and TNF-α levels were reduced in a dose-dependent manner, comparable to the suppression observed in LPS-treated cells. Notably, among all compounds tested, compounds 1–12 inhibited IL-6 levels compared to the untreated control. In contrast, TNF-α secretion remained largely unchanged relative to the cell control, however, a few compounds, such as **AS2**, **AS4**, **AS5**, and **AS6**, did exhibit a slight increase, which could be explained by the heterogeneous cell population of the splenocytes (Fig. 2A,B). Given the above observations indicating that spirocyclic compounds do not exert pro-inflammatory effects, their potential anti-inflammatory activity was next evaluated using an *in vitro* inflammatory model. RAW264.7 macrophages were stimulated with LPS prior to compound exposure (Fig. 2C). ELISA analysis revealed that **AS2**, **AS4**, **AS5**, **AS6**, **AS7**, **AS8**, **AS9**, and **AS10** compounds significantly inhibited LPS-induced IL-6 production at 100 µM, suggesting an anti-inflammatory and inhibitory activity on macrophage responses.

3.5 AS8 and AS10 Spirocyclic Compounds Inhibit Immune Response via the JAK/STAT Pathway

The compounds induced significant IL-10 production in RAW264.7 macrophages, while some also inhibited IL-6 production (<200 pg/mL), thereby warranting further investigation. Previous studies have shown that spirocyclic salts can inhibit immune responses and, specifically, the JAK2/STAT3 pathway. The regulation of PD-L1 expression is known to be mediated by the JAK/STAT pathway, activated by cytokines released from immune cells. The JAK proteins are multi-domain proteins consisting of seven domains: the kinase domain (JH1), the pseudo-kinase domain (JH2), the Src-homology-2 domain (JH3–JH4), and the FERM domain (JH5–JH7) [19]. The four JAK isoforms (JAK1, JAK2, JAK3, and TYK2) are observed to play a crucial role in the transduction of cytokine-mediated signals through the JAK-STAT pathway and are expressed in nearly all cells. The specific JAK-STAT combinations determine the cytokine signaling pathways that mediate various immunological functions. It has been observed that JAK1 and JAK3 are critical for the signaling pathways of several interleukins, including IL-2, IL-4, IL-7, IL-9, IL-15, and IL-21. Conversely, JAK2 modulates IL-6 and gp130 cytokine signalling. To this end, our experimentally verified, non-toxic series of 12 benzimidazole-based spirocyclic compounds was selected for further investigation of their binding interactions with JAK proteins. Molecular docking was performed to gain molecular-level insights into how these compounds interact with different JAK isoforms, which is crucial for understanding their potential inhibitory mechanisms [3].

Molecular docking was performed on all **12** compounds with JAK1, JAK2, JAK3 and TYK2 proteins to elucidate their binding interactions. The top ten scoring molecules for each protein were identified, and the common candidates with the potential to bind strongly to all JAK isoforms were shortlisted. These included compounds **AS1**, **AS2**, **AS7**, **AS8**, **AS10**, **AS11**, and **AS12**. **Supplementary Table 3** provides the docking scores of these seven molecules with all JAK isoforms. It is evident that these compounds bind to JAK proteins with varying affinity. The binding scores for these top seven molecules ranged from –6.9 kcal/mol to –9.3 kcal/mol. Specifically, it is observed that all these molecules exhibited binding scores $\leq$–8.0 kcal/mol for JAK1 and JAK3 proteins, whereas compounds **11** and **12** have binding scores of –6.9 kcal/mol and –7.6

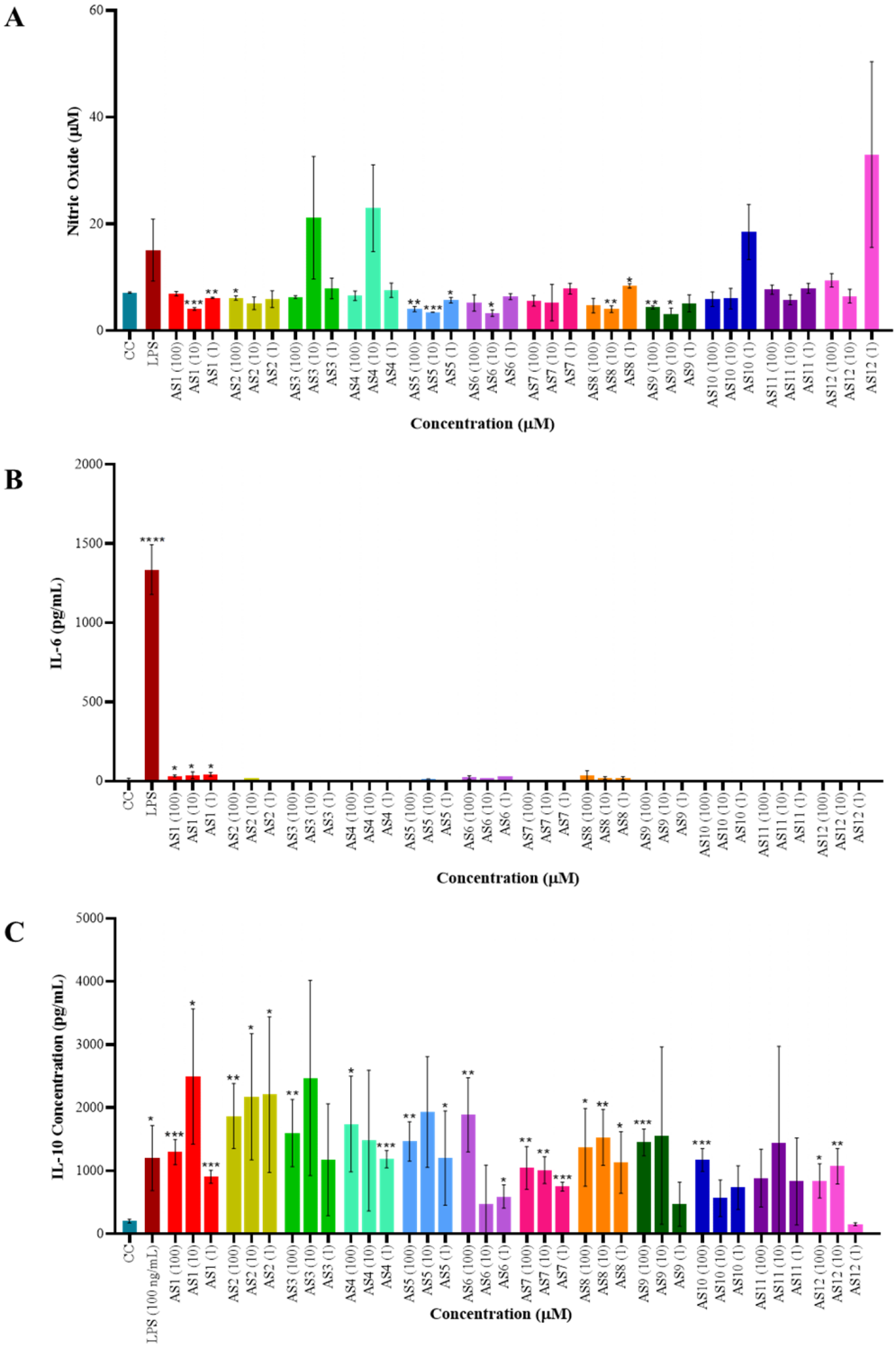

Fig. 1. Immunomodulatory activity of spirocyclic compounds—cytokine production analysis. (A) Nitric oxide (NO) production was assessed using the Griess reagent assay. RAW264.7 macrophages (0.5×10^6 cells/well) were incubated with the indicated compounds at 100 µM, 10 µM, or 1 µM for 24 hours (n = 3, technical replicates). (B,C) Cytokine quantification in naïve macrophages. Interleukin-6 (IL-6) (n = 3, technical replicates) and interleukin-10 (IL-10) (Biological replicates, n = 2; technical replicates, n = 3) levels in culture supernatants were determined by indirect sandwich enzyme-linked immunosorbent assay (ELISA), following 24 hours of treatment with compounds. lipopolysaccharide (LPS) (100 ng/mL) served as a positive control, and cell control (CC; untreated cells) as a negative control. Data are expressed as mean ± SD. Statistical analysis was performed between CC and compound-treated groups using an unpaired, non-parametric Student's *t*-test; * $p < 0.05$, ** $p < 0.01$, *** $p < 0.001$, and **** $p < 0.0001$ indicate the level of significance.

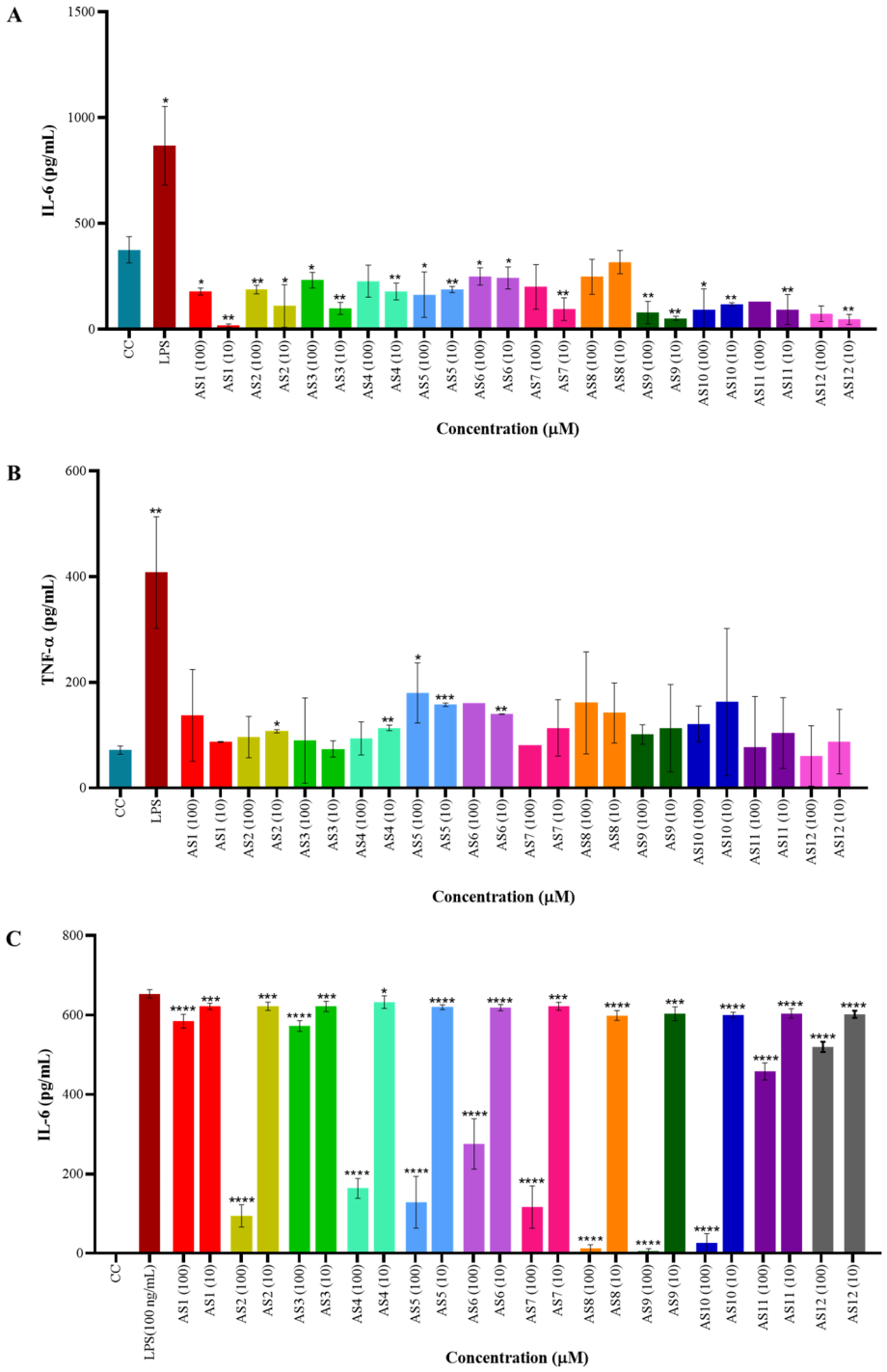

Fig. 2. Anti-inflammatory activity of spirocyclic compounds on murine splenocytes and RAW264.7 macrophages. (A,B) Quantification of pro-inflammatory cytokines IL-6 and tumor necrosis factor-alpha (TNF-α) in murine splenocyte cultures by indirect sandwich ELISA. Splenocytes (0.5×10^6 cells/well) were incubated with the indicated compounds at 100 µM or 10 µM for 24 hours (n = 3 biological replicates). LPS (100 ng/mL) served as a positive control, and cell control (CC; untreated cells) as a negative control. (C) Decrease of IL-6 secretion in RAW264.7 macrophages following LPS stimulation and compound treatment. Cells (0.5×10^6/well) were pre-incubated with LPS (100 ng/mL) for 2 hours, followed by treatment with spirocyclic compounds at 100 or 10 µM for 24 hours. Data represent two independent experiments (biological replicate = 2) performed in triplicate (n = 3, technical replicates). Data are expressed as mean ± SD. Statistical analysis was performed between CC and compound-treated groups (A,B) using an unpaired, non-parametric student's *t*-test; also statistical comparisons were made between LPS-treated and LPS + compound-treated groups (C) using an unpaired, non-parametric Student's *t*-test; * $p < 0.05$; ** $p < 0.01$; *** $p < 0.001$, and **** $p < 0.0001$ indicate the level of significance.

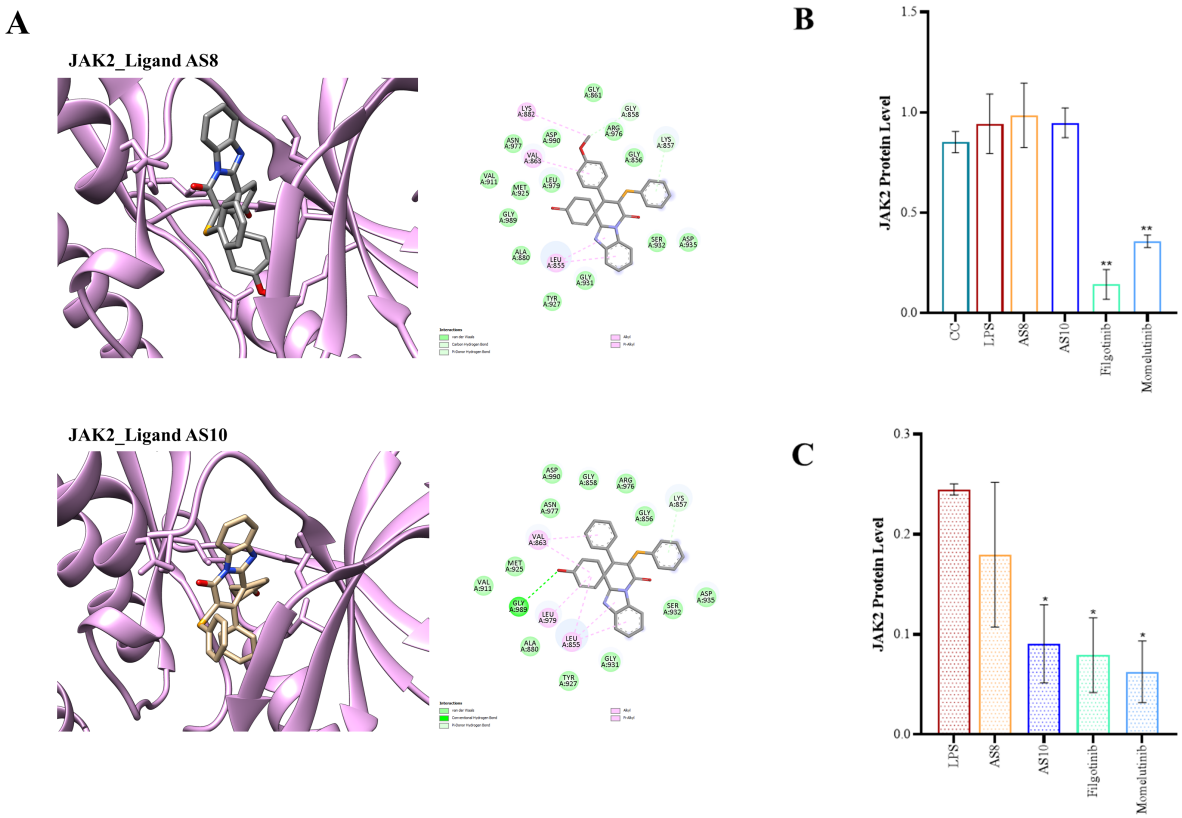

Fig. 3. ***In silico*** **molecular docking and** ***in vitro*** **evaluation of the interaction between JAK kinase and the spirocyclic compounds.** (A) The binding poses of compounds AS8 and AS10 in JAK2 proteins, along with corresponding 2D interaction maps. (B,C) Bar graph representation after quantification of JAK2 protein expression level in the murine macrophage cell line (All western blots, including uncropped, are available in the **Supplementary Information**). 0.5×10^6 cells/well were incubated with the indicated compounds at 100 μM for 24 hours with and without LPS stimulation for 2 hours (n = 2 biological replicates). Bar graph representation after quantification of JAK2 protein expression level. All data are expressed as mean ± SD. Statistical analysis was performed between CC and compound-treated groups for no LPS stimulation (B) and between LPS and compound-treated groups for LPS stimulation (C); using an unpaired, parametric Student's *t*-test; * $p < 0.05$ and ** $p < 0.01$ indicate the level of significance.

kcal/mol for JAK2 and TYK2 proteins, which are relatively low compared to the binding affinities of other compounds toward these proteins. Compounds **AS8** and **AS10** were consistently ranked among the top leads with high binding affinities (≤–8.0 kcal/mol), while **AS1** and **AS2** also demonstrated favorable interactions (≤–7.7 kcal/mol) across all four JAK isoforms [20]. To understand the molecular basis of these findings, the docking poses of these four compounds were further analyzed to identify specific hydrogen bonding and hydrophobic interactions.

The interaction analysis reveals that while both hydrogen, hydrophobic and pi interactions are present, the binding is majorly driven by hydrophobic interactions. A full summary of each of the compound **AS1**, **AS2**, **AS8**, and **AS10** interactions with all four isoforms is provided in the **Supplementary Table 4**. Moreover, Fig. 3A shows the binding pose for compounds **AS8** and **AS10** with the JAK2 protein, along with a 2D interaction map [20].

In silico docking, supported by prior inhibitory activity data, indicated that **AS1**, **AS2**, **AS8**, and **AS10** are potential inhibitors of the JAK/STAT pathway. To validate these findings, the expression of key genes and proteins involved in this pathway was evaluated following compound treatment. No significant changes were observed at the mRNA level (**Supplementary Fig. 1**). However, a pronounced reduction in total JAK2 protein expression was observed upon treatment with **AS8** and **AS10** (Fig. 3B,C and **Supplementary Fig. 2**). However, the phosphorylation status of JAK2 following compound treatment remains to be evaluated. In summary, **AS8** and **AS10** showed no cytotoxicity and significantly increased IL-10 while suppressing LPS-induced IL-6 in macrophages and splenocytes, indicating potent anti-inflammatory activity. Both compounds exhibited strong binding affinity to JAK isoforms (≤–8 kcal/mol) and reduced JAK2 protein expression. These findings suggest that selenium-containing scaffolds modulate inflammatory signaling pathways effectively.

4. Discussion

Previously, the *ipso*-annulation of benzimidazole-fused aza-spirocyclic compounds has been reported, demonstrating an effective strategy to enhance the structural and functional diversity of these molecules. Moreover, the azaspirocyclic framework is well represented among bioactive compounds. For example, Annosqualine contains a spirocycloheptadienone motif associated with notable cytotoxic activity, while Atiprimod, an orally bioavailable azaspiro compound, has advanced into clinical evaluation for cancer therapy. These precedents underscore the pharmacological relevance of azaspirocyclic scaffolds and further support their exploration as promising immunomodulatory chemotypes [4]. Due to the intriguing structural features and biological properties, this study proposed to identify immunomodulatory effects of those aza-spirocyclic compounds. We screened **12** aza-spirocyclic compounds, representing novel scaffolds designed and synthesized (**Supplementary Table 1**), with the expectation of exhibiting immunomodulatory properties. These immunotherapeutic compounds may have significant opportunities for exploring the vast possibilities targeting the aforementioned pathways and discovering small molecules as immunotherapeutics and/or vaccine adjuvants for cancer. Several spirocyclic analogues have been investigated for anti-inflammatory activity, yet only a few have progressed to clinical evaluation for autoimmune or inflammatory diseases. Beyond their anti-inflammatory potential, spirocyclic scaffolds have also been associated with antioxidant activity, highlighting their utility in the development of drug candidates for metabolic, neurodegenerative, and oncological conditions, including diabetes, Alzheimer's disease, and cancer [21].

Initially, the cytotoxicity of the synthesized compounds was assessed using an MTT assay in RAW264.7 macrophages. None of the compounds exhibited cytotoxic effects at concentrations exceeding 100 µM (**Supplementary Table 2**). To further evaluate their immunomodulatory potential, a series of assays, including NO quantification and cytokine profiling, were performed using both murine macrophages and murine splenocytes. No significant induction of NO and IL-6 was observed following treatment of RAW264.7 macrophages with any of the compounds. In contrast, a marked increase in IL-10 production was detected in response to the **AS1**, **AS2**, **AS3**, **AS4**, **AS5**, **AS6**, **AS8**, **AS9**, and **AS10** compounds. Similar trends were observed in murine splenocytes, which likewise showed no elevation or inhibition of pro-inflammatory cytokines (IL-6 and TNF-α), further supporting the absence of a pro-inflammatory response. To evaluate the immunosuppressive potential of the compounds, cytokine production was assessed under LPS-induced inflammatory conditions. Compounds **AS2**, **AS4**, **AS5**, **AS6**, **AS7**, **AS8**, **AS9**, and **AS10** inhibited LPS-stimulated IL-6 production, with the most pronounced suppression observed at levels below 200 pg/mL IL-6.

Moreover, the regulation of PD-L1 expression is known to be *via* activation of the JAK/STAT pathway by cytokines released by immune cells. Also, previously shown that spirocyclic salts depict inhibition of the immune and eventually JAK2/STAT3 pathway [3,22]. The specific JAK-STAT combinations determine the cytokine signaling pathways that mediate various immunological functions. It has been observed that JAK1 and JAK3 are critical for the signaling pathways of several interleukins, including IL-2, IL-4, IL-7, IL-9, IL-15, and IL-21 [3]. Conversely, JAK2 modulates IL-6 and gp130 cytokine signaling [3]. Additionally, *in silico* molecular docking revealed that four compounds; **AS1**, **AS2**, **AS8**, and **AS10**; exhibited strong binding affinity toward JAK proteins. To further validate these interactions, gene and protein expression analyses were performed. While no significant changes were observed at the mRNA level, **AS8** and **AS10** demonstrated inhibition of JAK2 at the total protein level. Furthermore, to exclude potential off-target effects, MAPK protein expression was evaluated and showed no significant changes (**Supplementary Fig. 3**). In contrast, we observed slightly elevated levels of IL-12p70, INF-γ, but not IL-10, production in murine dendritic cells (DCs) upon the treatment of the first series compounds (**Supplementary Fig. 4**). The enhanced activity observed for **AS8** and **AS10** may be associated with the presence of selenium; however, similar trends in other analogues indicate that the overall scaffold and substituent effects also contribute to the anti-inflammatory response. Selenium incorporation could influence redox properties and molecular interactions, potentially enhancing biological activity. Thus, the observed effects likely arise from a combination of structural features rather than selenium alone [1]. Therefore, to support our findings, further experiments are required to confirm the immunomodulatory activities of the compounds.

5. Limitations

The present study has several limitations. While spirocyclic architectures are progressively getting popular in drug discovery for their three-dimensional shape, rigidity, and potential to improve pharmacological profiles, they possess significant limitations related to synthetic complexity, structural stability, and physicochemical properties. The immunological assessment was confined to a limited set of cytokines (IL-6, TNF-α, and IL-10) and nitric oxide production, thereby providing only a partial understanding of the immunomodulatory effects. Further evaluation of additional cytokines, such as IFN-γ and TGF-β, is necessary to achieve a more comprehensive understanding and to experimentally validate the involvement of the JAK/STAT signaling pathway. Also, the functional pathway validation, including the phosphorylation status of JAK/STAT proteins, is to be studied. Moreover, the find-

ings are based on *in vitro*, *ex vivo*, and *in silico* models, which may not fully recapitulate *in vivo* immune responses. Future investigations are therefore required to address these aspects and to further substantiate the therapeutic potential of these compounds.

6. Conclusion

The newly synthesized aza-spirocyclic compounds showed excellent cytocompatibility and clear immunomodulatory potential. A subset of five compounds increased IL-10 while suppressing LPS-induced IL-6, indicating strong anti-inflammatory and immunosuppressive activity. Combined with their predicted affinity for JAK proteins, these findings suggest that aza-spirocyclic scaffolds may modulate JAK/STAT-related pathways. Among the series of compounds, **AS8** and **AS10** represent promising anti-inflammatory candidates, demonstrating favorable cytokine modulation and interaction with inflammatory signaling pathways. While selenium-containing derivatives showed notable activity, further structure-activity relationship studies are required to delineate the specific contribution of selenium. These compounds provide a useful framework for future optimization of immunomodulatory agents.

Availability of Data and Materials

All data associated with this study are included in this publication. The synthesized molecules are available at the R.R.C. The datasets used and analyzed during the current study are available from the corresponding author on reasonable request.

Author Contributions

SRB and RRC designed and supervised the study. RRC synthesized and characterized the compounds. AP performed the biology research and analyzed the data. RRT performed the molecular docking and immuno-informatics analysis. SRB and RRC performed the analysis and wrote the manuscript with the input from all the authors. All authors contributed to editorial changes in the manuscript. All authors read and approved the final manuscript. All authors have participated sufficiently in the work and agreed to be accountable for all aspects of the work.

Ethics Approval and Consent to Participate

All animal experiments were conducted in accordance with the guidelines of the Institutional Animal Ethics Committee (IAEC), CSIR-IICT, Hyderabad, India, and were approved under protocol number IICT-IAEC-069-2025. This study adhered to the animal welfare guidelines of the Committee for Control and Supervision of Experiments on Animals (CCSEA), Government of India.

Acknowledgment

SRB would like to thank the director, CSIR-Indian Institute of Chemical Technology, Hyderabad, for providing infrastructure, lab space, and support for an institutional research grant (MLP9033). CSIR-IICT manuscript communication number: IICT/Pubs./2025/443. AP would like to thank Poornima Penta for guiding in ELISA experiment and Srilekha Paidighantam for helping during splenocyte harvesting. S.R.B would like to thank Anusandhan National Research Foundation (ANRF) for the award of Prime Minister Early Career Research Grant: ANRF/ECRG/2024/000505/LS. S.R.B. thanks Ignite Life Science Foundation (https://ignitelsf.in/) for the award of the grant: Acorn-AMR3/RNATech/2024/01. R.R.T acknowledges DST for providing the INSPIRE Faculty Fellowship and research grant (IFA-23-PH-308).

Funding

This project was supported by the CSIR, Grant No. CSPS24/RDSF/IICT/IHP24/01. AP was supported by the ICMR-JRF fellowship of the Department of Health Research, New Delhi, India (Award Number-3/1/3/JRF-2023/HRD - 046(145819)).

Conflicts of Interest

The authors declare no conflicts of interest. Given his role as the Guest Editor, Srinivasa Reddy Bonam had no involvement in the peer-review of this article and has no access to information regarding its peer review. Full responsibility for the editorial process for this article was delegated to Changqing Su.

Declaration of AI and AI-Assisted Technologies in the Writing Process

ChatGPT GO was used to correct grammar and improve the language of the manuscript. After using this tool, the authors reviewed and edited the content as needed and take full responsibility for the content of the publication.

Supplementary Material

Supplementary material associated with this article can be found, in the online version, at https://doi.org/10.31083/FBL48867.

References

[1] Kim MK, Shin H, Park KS, Kim H, Park J, Kim K, *et al.* Benzimidazole Derivatives as Potent JAK1-Selective Inhibitors. Journal of Medicinal Chemistry. 2015; 58: 7596–7602. https://doi.org/10.1021/acs.jmedchem.5b01263.

[2] Bansal Y, Silakari O. The therapeutic journey of benzimidazoles: a review. Bioorganic & Medicinal Chemistry. 2012; 20: 6208–6236. https://doi.org/10.1016/j.bmc.2012.09.013.

[3] Hu X, Li J, Fu M, Zhao X, Wang W. The JAK/STAT signaling pathway: from bench to clinic. Signal Transduction and Targeted Therapy. 2021; 6: 402. https://doi.org/10.1038/s41392-021-00791-1.

[4] Reddy CR, Ajaykumar U, Kolgave DH, Ramesh R. CAN-Promoted Thiolative *ipso*-Annulation of Unactivated *N*-Benzyl Acrylamides: Access to SCN/SCF_3/SO_2Ar Containing Azaspirocycles. The Journal of Organic Chemistry. 2023; 88: 7117–7127. https://doi.org/10.1021/acs.joc.3c00374.

[5] Reddy CR, Srinivasu E, Subbarao M. Seleno/Thio-functionalized ipso-Annulation of N-Propiolyl-2-arylbenzimidazole to Construct Azaspiro[5,5]undecatrienones. The Journal of Organic Chemistry. 2023; 88: 16485–16496. https://doi.org/10.1021/acs.joc.3c01991.

[6] Swetha K, Bhatnagar A, Lakavathu M, Poornima P, Ganesh P, Kamath A, *et al*. Biological degradation of graphitic carbon nitride sheets and autophagy induction in macrophages. Nanoscale. 2025; 17: 15267–15278. https://doi.org/10.1039/d5nr00795j.

[7] Houdkova M, Rondevaldova J, Doskocil I, Kokoska L. Evaluation of antibacterial potential and toxicity of plant volatile compounds using new broth microdilution volatilization method and modified MTT assay. Fitoterapia. 2017; 118: 56–62. https://doi.org/10.1016/j.fitote.2017.02.008.

[8] Pratama RR, Sari RA, Sholikhah I, Mansor H, Chang HI, Sukardiman, *et al*. Inhibition of nitric oxide production in RAW 264.7 cells and cytokines IL-1β in osteoarthritis rat models of 70 % ethanol extract of *Arcangelisia flava* (L.) merr stems. Heliyon. 2024; 10: e35730. https://doi.org/10.1016/j.heliyon.2024.e35730.

[9] Bonam SR, Bhunia D, Muller S, Nerella SG, Alvala M, Halmuthur Mahabalarao SK. Novel trisaccharide based phospholipids as immunomodulators. International Immunopharmacology. 2019; 74: 105684. https://doi.org/10.1016/j.intimp.2019.105684.

[10] Kubo A, Minamino N, Isumi Y, Katafuchi T, Kangawa K, Dohi K, *et al*. Production of adrenomedullin in macrophage cell line and peritoneal macrophage. The Journal of Biological Chemistry. 1998; 273: 16730–16738. https://doi.org/10.1074/jbc.273.27.16730.

[11] Al-Jadani S. Molecular Docking and Dynamics Analysis of Tofacitinib Binding to JAK1: Implications for Autoimmune Disorder Therapy. Ain Shams Medical Journal. 2024; 75: 808–821. https://doi.org/10.21608/asmj.2024.319125.1311.

[12] Faris A, Cacciatore I, Alnajjar R, Hanine H, Aouidate A, Mothana RA, *et al*. Revealing innovative JAK1 and JAK3 inhibitors: a comprehensive study utilizing QSAR, 3D-Pharmacophore screening, molecular docking, molecular dynamics, and MM/GBSA analyses. Frontiers in Molecular Biosciences. 2024; 11: 1348277. https://doi.org/10.3389/fmolb.2024.1348277.

[13] Sathish S, Devaraju P, Julius A, Sohn H, Madhavan T. Identification of selective inhibitors for Janus kinase 1: an integrated drug repurposing strategy for breast cancer. Chemical Papers. 2024; 78: 245–262. https://doi.org/10.1007/s11696-023-03070-1.

[14] Chandrasekhar B, Sohn H, Madhavan T. Discovery of potential JAK2 inhibitor: In silico molecular docking and molecular dynamics study for colon cancer therapy. Chemical Papers. 2025; 79: 5319–5334. https://doi.org/10.1007/s11696-025-04127-z.

[15] Faris A, Cacciatore I, Alnajjar R, Aouidate A, Al Mughram MH, Elhallaoui M. Computational insights into rational design and virtual screening of pyrazolopyrimidine derivatives targeting Janus kinase 3 (JAK3). Frontiers in Chemistry. 2024; 12: 1425220. https://doi.org/10.3389/fchem.2024.1425220.

[16] Hiesinger K, Dar'in D, Proschak E, Krasavin M. Spirocyclic Scaffolds in Medicinal Chemistry. Journal of Medicinal Chemistry. 2021; 64: 150–183. https://doi.org/10.1021/acs.jmedchem.0c01473.

[17] Dunbar KL, Scharf DH, Litomska A, Hertweck C. Enzymatic Carbon-Sulfur Bond Formation in Natural Product Biosynthesis. Chemical Reviews. 2017; 117: 5521–5577. https://doi.org/10.1021/acs.chemrev.6b00697.

[18] Ernst O, Glucksam-Galnoy Y, Bhatta B, Athamna M, Ben-Dror I, Glick Y, *et al*. Exclusive Temporal Stimulation of IL-10 Expression in LPS-Stimulated Mouse Macrophages by cAMP Inducers and Type I Interferons. Frontiers in Immunology. 2019; 10: 1788. https://doi.org/10.3389/fimmu.2019.01788.

[19] Galvez-Llompart M, Ocello R, Rullo L, Stamatakos S, Alessandrini I, Zanni R, *et al*. Targeting the JAK/STAT Pathway: A Combined Ligand- and Target-Based Approach. Journal of Chemical Information and Modeling. 2021; 61: 3091–3108. https://doi.org/10.1021/acs.jcim.0c01468.

[20] Bono A, La Monica G, Alamia F, Lauria A, Martorana A. A novel in silico approach for identifying multi-target JAK/STAT inhibitors as anticancer agents. Journal of Molecular Graphics & Modelling. 2025; 135: 108913. https://doi.org/10.1016/j.jmgm.2024.108913.

[21] Acosta-Quiroga K, Rojas-Peña C, Nerio LS, Gutiérrez M, Polo-Cuadrado E. Spirocyclic derivatives as antioxidants: a review. RSC Advances. 2021; 11: 21926–21954. https://doi.org/10.1039/d1ra01170g.

[22] Zhang W, Sun Q, Gao X, Jiang Y, Li R, Ye J. Anti-inflammation of spirocyclopiperazinium salt compound LXM-10 targeting α7 nAChR and M4 mAChR and inhibiting JAK2/STAT3 pathway in rats. PLoS ONE. 2013; 8: e66895. https://doi.org/10.1371/journal.pone.0066895.